Don't Judge the Moon by its Cover: Getting Below the Surface with Mini-RF

Angela M. Stickle, G. Wes Patterson, Lauren M. Jozwiak, Anna C. Martin, Cole A. Nypaver
and the Mini-RF Team (Angela.Stickle@jhuapl.edu)

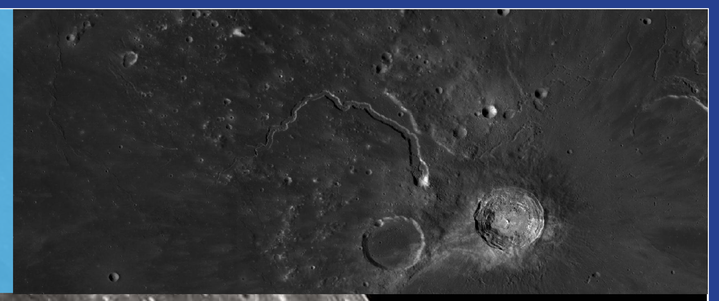

Mini-RF Bistatic Operations

- Mini-RF is a dual-frequency radar flying onboard the Lunar Reconnaissance Orbiter (LRO) and is currently operating in a bistatic configuration with Arecibo Observatory in Puerto Rico and the DSS-13 antenna at Goldstone acting as transmitters. Mini-RF receives the signal backscattered from the lunar surface.
- DSS-13 is used for the collection of X-band (7147 MHz; 4.2 cm) data
- Arecibo Observatory is used for the collection of S-band (2380 MHz; 12.6 cm) data
- Mini-RF receives orthogonal linear polarizations (H and V).
- The circular polarization ratio, CPR = $(S_1-S_4)/(S_1+S_4)$, is one Mini-RF data product (right) that it is commonly used in analyses of planetary radar data [1,2]. This ratio provides an indication of surface roughness, as determined by the distribution of surface and buried wavelength-scale scatterers (e.g., boulders).

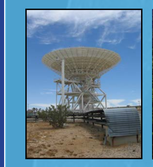

The Aristarchus Plateau

- On the lunar nearside, characterized by many interesting geological features
- Surrounded by flood basalts of Oceanus Procellarum (below, panel D), is oddly shaped, and has extreme high and low reflectance areas (e.g., below, panel A).
- The rille, Vallis Schröter, cuts through the plateau, which is also nearly covered by a large pyroclastic deposit thought to be between 20-30m thick (below, panel C) [3] and dominated by low-Ti glass spheroids [e.g., 4-5].
- A set of streaks, which are generally radial to Aristarchus crater, have been observed in multiple wavelengths (e.g., optical, radar) across the plateau. (bottom)

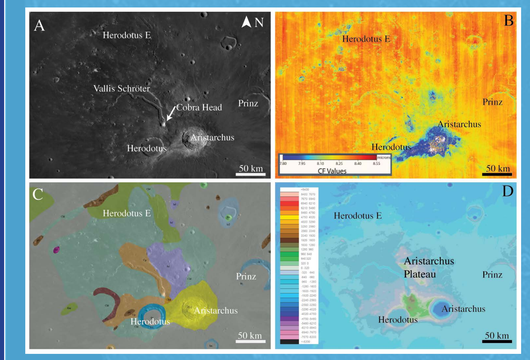

Mini-RF Obervations Showcase Aristarchus in a New Way

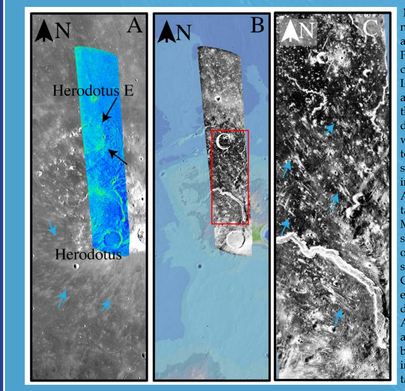

Mini-RF CPR (roughness) (λ=12.6 cm) image of the Aristarchus Plateau and Herodotus crater, overlain on the LROC WAC image. Black arrows show the rim of the ancient crater Herodotus E (48 km dia.), which is often difficult to identify in other data sets, while blue arrows indicate streaks radial to Aristarchus crater. B) Total power returned to the Mini-RF radar from backscattered energy overlain on the LDEM256 radar shaded topography. C) Close-up of (B) indicated by a red box: Mini-RF data for a portion of the Aristarchus Plateau. Blue arrows indicate radar bright streaks approximately radial to Aristarchus crater.

New Mini-RF Obervations

Mini-RF observed the Aristarchus plateau region 3 times in bistatic geometry since 2012.

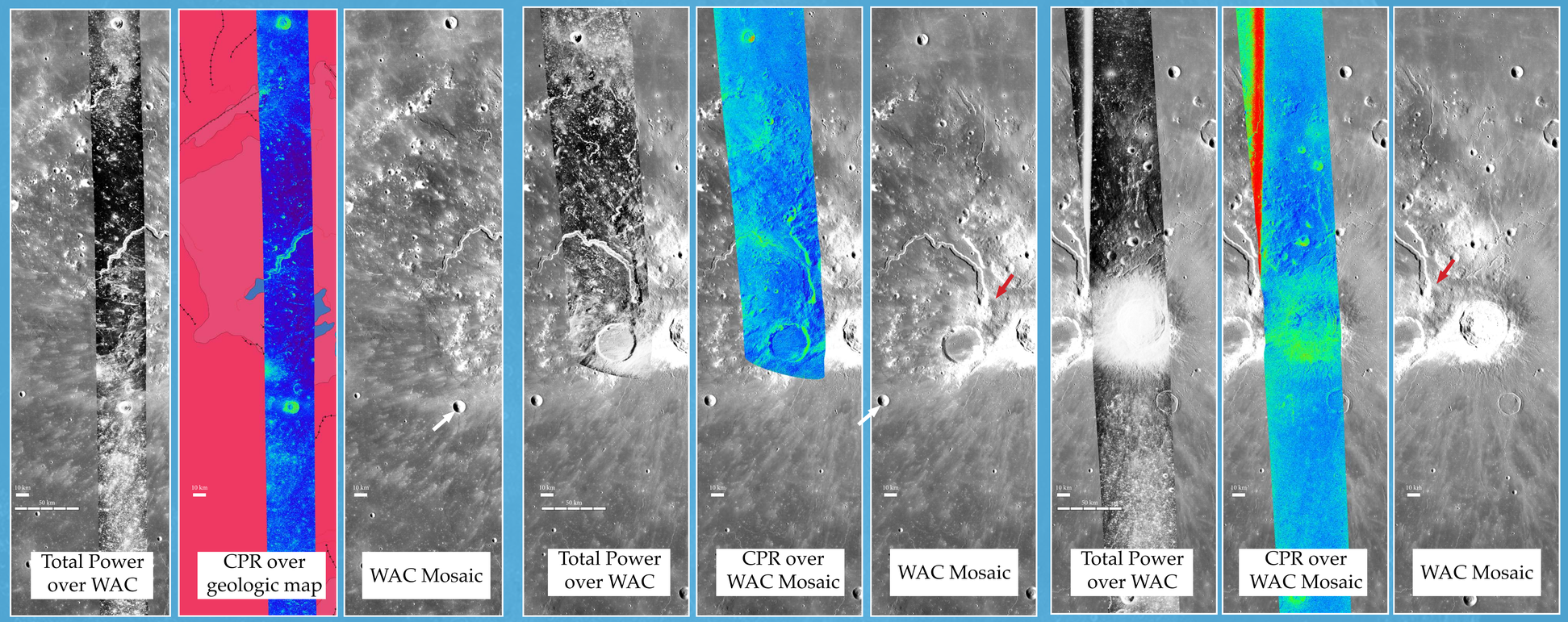

The Mini-RF team is releasing newly reprocessed data and additional products into the PDS to accompany the bistatic data

Mini-RF data quality has been improved:

- Temperature dependent calibration included in processed data
- Geometry and timing updated in data processor to decrease and/or remove along-track offset of Mini-RF data products (right)
- Updates to the Mini-RF processor to include improved direct path phase model and antenna pattern

(right) Updates to the Mini-RF bistatic data processor improve georegistration of the Mini-RF data products. (top) Original processing resulted in along-track and across-track errors. Here, a 2-km bias is correctd, but the data are still not registered with the DEM. (bottom) Registration is significantly improved with new processing imrovements

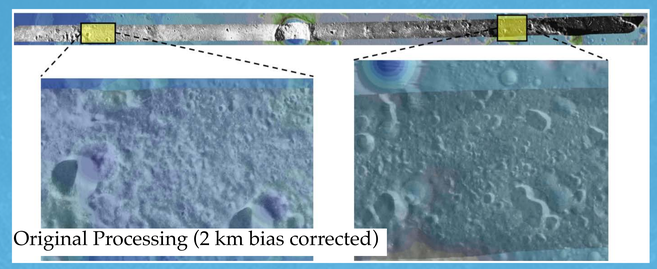

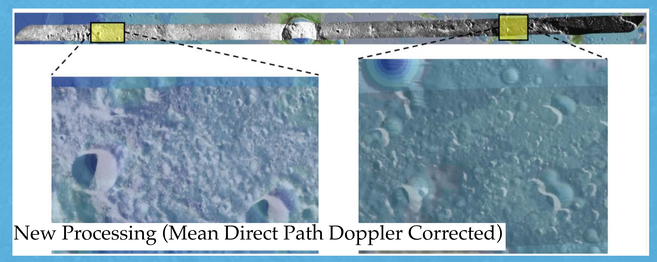

New data products include:

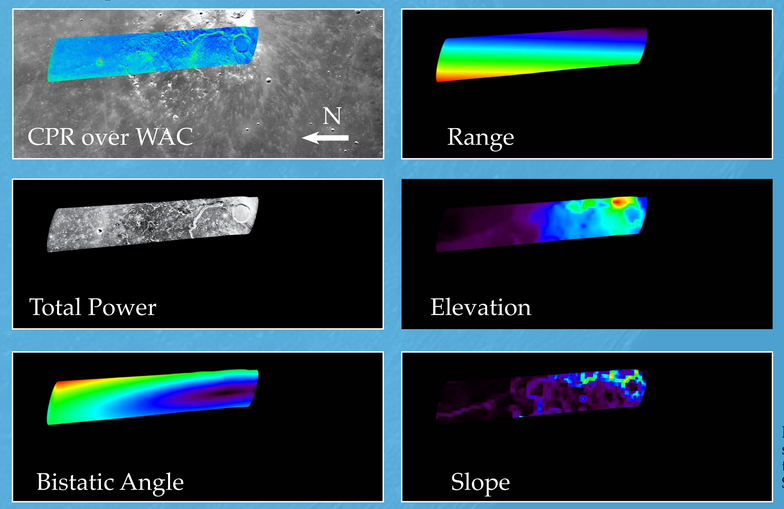

- Additional backplanes for analysis, including: latitude, longitude, incidence angle, emission angle, bistatic angle, range, slope, elevation (left)
- Photoshop files that include widely used data products (total power and CPR) overlain on other data for context and easier evaluation, including:
  - WAC imagery
  - New unified global geologic map (above)
  - DEMs (radar and image derived)

Newly reprocessed bistatic will be put into the PDS later this year. Stay tuned!

[1] Campbell et al. (2010), Icarus, 208, 565-573; [2] Raney et al. (2012), JGR, 117, E00H21; [3] McEwen et al. (1994) Science, 266, 1858–1862; [4] Lucey et al. (1986) Proc. Lunar and Planet. Sci. Conf. 16th, J. Geophys. Res., 91, Suppl., D344–D354; [5] Mustard et al. (2011), J. Geophys. Res. Planets